ヘレ・ショウ流れ，結晶成長，紙の燃焼に対する境界追跡法について[1)]
On boundary tracking methods for Hele-Shaw flows, crystal growth and combustion of paper

明治大学理工学部　矢崎 成俊 (Shigetoshi YAZAKI)
School of Science and Technology, Meiji University[2)]

Abstracts. A simple and fast numerical methods for the classical Hele-Shaw problem, the area-preserving crystalline curvature flow equation, and the closed curve version of Kuramoto-Sivashinsky equation are presented.

1 Introduction

Let $\mathcal{C}(t)$ be a smooth Jordan curve at time t in the plane $\mathbb{R}^2$. In the physical context, $\mathcal{C}(t)$ is a model of interface between a viscous liquid and the air, boundary of crystal, a flame/smoldering front, and so on. The curve $\mathcal{C}(t)$ is parameterized by $\boldsymbol{x}(u,t)$ for $u \in [0,1]$ and moves by

$$\dot{\boldsymbol{x}}(u,t) = V(u,t)\boldsymbol{N}(u,t) + W(u,t)\boldsymbol{T}(u,t), \tag{1.1}$$

where $\dot{\mathsf{F}} = \partial \mathsf{F}/\partial t$.

In this paper we follow the so-called direct approach in which the evolution of the position vector $\boldsymbol{x} = \boldsymbol{x}(u,t)$ is governed by equation (1.1), especially in the case where the normal $\boldsymbol{N}$ velocity V is given by the following equations: one phase Hele-Shaw flow equation, crystalline curvature flow equation, and Kuramoto-Sivashinsky equation, while the tangent $\boldsymbol{T}$ velocity W controls the grid-point spacing to be uniform. Note that the tangential velocity W has no effect on the shape of evolving curve, which is determined by the value of the normal velocity V only. Therefore, one can take $W \equiv 0$ when analyzing analytical properties of the geometric flow driven by (1.1). On the other hand, the impact of a suitable choice of W on the construction of robust and stable numerical schemes has been pointed out by many authors (see e.g., [9, 14] and references therein).

2 Moving Jordan curve and eight examples

Time evolution of a Jordan curve $\mathcal{C}(t)$ is parameterized by $\boldsymbol{x} : [0,1] \times [0,T) \to \mathbb{R}^2$ s.t. $\mathcal{C}(t) = \{\boldsymbol{x}(u,t); u \in [0,1]\}$ and $|\boldsymbol{x}'| > 0$. Here $\boldsymbol{x}' = \partial \boldsymbol{x}/\partial u$ and $g(u,t) = |\boldsymbol{x}'|$ is the local length. We denote $|\boldsymbol{a}| = \sqrt{\boldsymbol{a}\cdot\boldsymbol{a}}$ where $\boldsymbol{a}\cdot\boldsymbol{b}$ is the inner product between $\boldsymbol{a}$ and $\boldsymbol{b} \in \mathbb{R}^2$. The unit tangent vector is $\boldsymbol{T} = \boldsymbol{x}'/g = \boldsymbol{x}_s$ where s is the arc-length parameter $ds = g\,du$ and $\mathsf{F}_s = \mathsf{F}'/g$, i.e., $\partial/\partial s = g^{-1}\partial/\partial u$ is the formal definition, since the arc-length s depends on u and t. The unit outward normal vector is $\boldsymbol{N} = -\boldsymbol{T}^{\perp}$ where $(a,b)^{\perp} = (-b,a)$. The tangential angle θ is defined s.t. $\boldsymbol{T} = (\cos\theta, \sin\theta)^{\mathrm{T}}$. The curvature κ is obtained from $\boldsymbol{T} = \boldsymbol{x}_s$ and the Frenét formula $\boldsymbol{T}_s = -\kappa\boldsymbol{N}$, from which it follows that $\kappa = \theta_s$ or $\kappa = \det(\boldsymbol{x}_s, \boldsymbol{x}_{ss})$ where $\mathsf{F}_{ss} = (\mathsf{F}'/g)'/g$ (sign convention is the way that $\kappa = 1$ if $\mathcal{C}$ is a unit circle). See Figure 2.1.

[1)] Manuscript for 『数値解析学の最前線：理論・方法・応用』, November 8–10, 2017 at RIMS, Kyoto University. This work was partially supported by KAKENHI No.16H03953.

[2)] 1-1-1 Higashi-Mita, Tama-ku, Kanagawa 214-8571, Japan. *E-mail*: syazaki@meiji.ac.jp

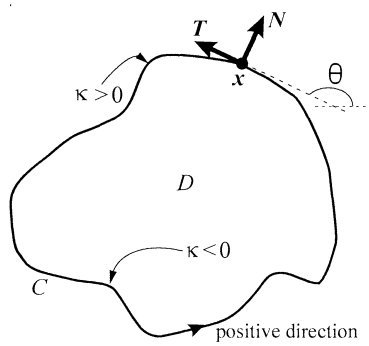

Figure 2.1: Moving Jordan curve

A geometric evolution problem can be formulated as follows: For a given initial Jordan curve $\mathcal{C}^0$, find a family of curves $\{\mathcal{C}(t)\}_{0\le t<T}$, starting from $\mathcal{C}(0)=\mathcal{C}^0$ and evolving by the normal velocity V.

In what follows, we show eight examples of various kinds of the normal velocity V.

Example 2.1 A simple example of V is the **Eikonal equation** $V=-1$, which is the L^2-gradient flow of the enclosed area $\mathcal{A}(t)=\dfrac{1}{2}\int_{\mathcal{C}(t)}\boldsymbol{x}\cdot\boldsymbol{N}\,ds$, since

$$\dot{\mathcal{A}}(t)=\int_{\mathcal{C}(t)}V\,ds. \tag{2.1}$$

Example 2.2 Another typical example is the classical **curvature flow equation** $V=-\kappa$, which is the L^2-gradient flow of the total length $\mathcal{L}(t)=\int_{\mathcal{C}(t)}ds$, since

$$\dot{\mathcal{L}}(t)=\int_{\mathcal{C}(t)}\kappa V\,ds. \tag{2.2}$$

Then we have the curve-shortening property (**CS-property** in short) $\dot{\mathcal{L}}(t)\le 0$, and then $V=-\kappa$ is also called the curve-shortening equation.

Example 2.3 The **area-preserving curvature flow equation** $V=\langle\kappa\rangle-\kappa$ is also classical, where $\langle\mathsf{F}\rangle=\mathcal{L}(t)^{-1}\int_{\mathcal{C}(t)}\mathsf{F}\,ds$ is the average of F along the curve $\mathcal{C}(t)$. The enclosed area $\mathcal{A}(t)$ is preserved in time (**AP-property** in short), since from (2.1) we have

$$\dot{\mathcal{A}}(t)=\int_{\mathcal{C}(t)}(\langle\kappa\rangle-\kappa)\,ds=\langle\kappa\rangle\int_{\mathcal{C}(t)}ds-\int_{\mathcal{C}(t)}\kappa\,ds=0.$$

By means of CBS inequality, we also have the CS-property $\dot{\mathcal{L}}\le 0$ which is the same as the classical curvature flow equation $V=-\kappa$ in Example 2.2. Indeed, $V=\langle\kappa\rangle-\kappa$ is the L^2-gradient flow of $\mathcal{L}$ subject to area-preserving.

Example 2.4 The fourth example is the **Willmore flow equation** $V=\kappa_{ss}+\kappa^3/2$, which is the L^2-gradient flow of the elastic energy $\mathcal{E}(t)=\int_{\mathcal{C}(t)}\kappa^2\,ds/2$, since

$$\dot{\mathcal{E}}(t)=-\int_{\mathcal{C}(t)}\left(\kappa_{ss}+\frac{1}{2}\kappa^3\right)V\,ds. \tag{2.3}$$

Example 2.5 The fifth example is the **surface diffusion flow equation** $V = \kappa_{ss}$ which is formally obtained from the Willmore flow equation without the term $\kappa^3/2$. The solution of this equation satisfies the AP-property $\dot{\mathcal{A}}(t) = \int_{\mathcal{C}(t)} \kappa_{ss}\, ds = 0$. We also have the CS-property $\dot{\mathcal{L}}(t) \leq 0$, and in this sense, the surface diffusion flow and the area-preserving curvature flow are very similar each other.

Example 2.6 As we have seen, the area-preserving curvature flow equation $V = \langle\kappa\rangle - \kappa$ and the surface diffusion flow equation $V = \kappa_{ss}$ have the AP- and the CS-properties. The following **Hele-Shaw flow equation** also has these two properties.

The Hele-Shaw problem is description of a motion of viscous fluid in a quasi two-dimensional space, which was starting from a short paper [5] in 1898 by Henry Selby Hele-Shaw (1854–1941). In his experiment, viscous fluid is sandwiched between two parallel plates with a narrow gap, and the apparatus is called Hele-Shaw cell. He succeeded to visualize stream lines by means of colored water in the cell. In the mathematical context, the Hele-Shaw problem is reduced from Navier-Stokes equations via stationary Stokes approximation, parabolic-shape approximation of the velocity profile, and assumption of the Laplace relation on the boundary, that is, the problem is stated as follows (see [8, 4] in detail):

$$\begin{cases} \triangle p = 0 & \text{in } \mathcal{D}(t), \\ p = \gamma\kappa & \text{on } \mathcal{C}(t), \\ V = -\nabla p \cdot \boldsymbol{N} & \text{on } \mathcal{C}(t), \end{cases} \tag{2.4}$$

where $\mathcal{D}(t) \subset \mathbb{R}^2$ is region occupied by fluid, $\mathcal{C}(t) = \partial\mathcal{D}(t)$ is the boundary, p is the pressure function, κ is the curvature, $\gamma > 0$ is the surface tension coefficient, $\boldsymbol{N}$ is the unit outward normal vector, and $V = \dot{\boldsymbol{x}} \cdot \boldsymbol{N}$ is the normal velocity. See Figure 2.1.

Thus the Hele-Shaw problem is stated as a kind of moving boundary problems determining unknown function p and unknown fluid region $\mathcal{D}$. It can be described in another way such as follows. Let $\boldsymbol{u}$ be the velocity vector of two-dimensional fluid. Then the harmonicity of the pressure p is an expression of continuation derived from the Darcy's law $\boldsymbol{u} = -\nabla p$ and the incompressible condition of fluid $\operatorname{div} \boldsymbol{u} = 0$, and the normal velocity V is derived from mass conservation law $\dot{\boldsymbol{x}} = \boldsymbol{u}$.

When the pressure p and the curve $\mathcal{C}(t)$ are solutions of the Hele-Shaw problem (2.4), then we have the CS-property in the following sense

$$-\dot{\mathcal{L}}(t) = \frac{1}{\gamma}\int_{\mathcal{C}(t)} p\nabla p \cdot \boldsymbol{N}\, ds = \frac{1}{\gamma}\iint_{\mathcal{D}(t)} \operatorname{div}(p\nabla p)\, dxdy = \frac{1}{\gamma}\iint_{\mathcal{D}(t)} |\nabla p|^2\, dxdy \geq 0.$$

We also have the AP-property

$$\dot{\mathcal{A}}(t) = -\int_{\mathcal{C}(t)} \nabla p \cdot \boldsymbol{N}\, ds = -\iint_{\mathcal{D}(t)} \operatorname{div}(\nabla p)\, dxdy = -\iint_{\mathcal{D}(t)} \triangle p\, dxdy = 0.$$

Example 2.7 Let us consider the total interfacial energy $\mathcal{L}_\sigma(t) = \int_{\mathcal{C}(t)} \sigma(\theta)\, ds$, where $\sigma > 0$ is the interfacial energy density per unit arc-length and θ is the tangential angle as

in Figure 2.1. Then the L^2-gradient flow of $\mathcal{L}_\sigma$ is $V = -\kappa_\sigma$, where $\kappa_\sigma = (\sigma + \sigma'')\kappa$ is the weighted curvature, since we have

$$\dot{\mathcal{L}}_\sigma(t) = \int_{\mathcal{C}(t)} \kappa_\sigma V \, ds, \tag{2.5}$$

which is regarded as the anisotropic version of (2.2). The equation $V = -\kappa_\sigma$ is called the **weighted curvature flow equation**. The energy density σ is specified by so-called the Wulff shape $\mathcal{W}_\sigma = \bigcap_{\theta\in[0,\pi]} \{\boldsymbol{x} \in \mathbb{R}^2;\ \boldsymbol{x} \cdot \boldsymbol{N}(\theta) \le \sigma(\theta)\}$, where $\boldsymbol{N}(\theta) = (\sin\theta, -\cos\theta)^{\mathrm{T}}$. If σ is a smooth function of θ and $\sigma + \sigma''$ is positive, then $(\sigma + \sigma'')^{-1}$ is the curvature of the boundary of the Wulff shape $\mathcal{W}_\sigma$. When the Wulff shape is a polygon, σ is not smooth and is called crystalline energy density, and the gradient flow of total crystalline energy derive the so-called **crystalline curvature flow equation**, which will be discussed in §5.

Example 2.8 The last example is the case where the normal velocity V is a linear combination of the Eikonal, the classical curvature flow and the surface diffusion flow equations with the coefficients $V^{(0)}$, $\alpha_{\mathrm{eff}} - 1$ and δ such that

$$V = V^{(0)} + (\alpha_{\mathrm{eff}} - 1)\kappa + \delta\kappa_{ss}, \tag{2.6}$$

where $V^{(0)}$ is a constant speed, and α_{eff} and δ are positive parameters. This equation (2.6) is equivalent to, in a certain scale, the so-called **Kuramoto-Sivashinsky equation** for the graph $y = f(x,t)$ of a curved flame front [7, 15] when $V^{(0)} = 1$ and $\delta = 4$:

$$\dot{f} + \frac{1}{2}f'^2 + (\alpha_{\mathrm{eff}} - 1)f'' + 4f'''' = 0, \tag{2.7}$$

where $f' = \partial f/\partial x$, $f'' = \partial^2 f/\partial x^2$ and $f'''' = \partial^4 f/\partial x^4$. One can find the simple scaling argument in [3].

If $\alpha_{\mathrm{eff}} > 1$, then $(\alpha_{\mathrm{eff}} - 1)\kappa$ induces instability, which is similar to the ill-posedness of backward heat equation $\dot{f} = -f''$, and $\delta\kappa_{ss}$ plays a stabilization role of the unstable front. An alternative stabilization method is to use the Willmore flow [10].

3 Numerical scheme for (1.1)

In the direct approach, a moving Jordan curve is approximated by a moving Jordan polygonal curve, say $\Gamma(t)$ at time t, with N vertices labeled $\boldsymbol{x}_1, \boldsymbol{x}_2, \cdots, \boldsymbol{x}_N$ in the anticlockwise order. Let Γ_i be the i-th edge $\Gamma_i = [\boldsymbol{x}_{i-1}, \boldsymbol{x}_i]$ ($i = 1, 2, \cdots, N$; $\boldsymbol{x}_0 = \boldsymbol{x}_N$). Then the moving Jordan polygonal curve at time t is $\Gamma(t) = \bigcup_{i=1}^N \Gamma_i(t)$. Our goal here is to construct a discretization of (1.1) in space, i.e., to derive a system of ordinary differential equations (ODEs in short) for $\Gamma(t)$: for $i = 1, 2, \cdots, N$

$$\dot{\boldsymbol{x}}_i(t) = V_i(t)\boldsymbol{N}_i(t) + W_i(t)\boldsymbol{T}_i(t), \tag{3.1}$$

where V_i is the normal $\boldsymbol{N}_i$-component of the velocity at $\boldsymbol{x}_i$, and W_i the tangential $\boldsymbol{T}_i$-component of the velocity at $\boldsymbol{x}_i$.

The right-hand-side of (3.1) consists of several polygonal quantities on Γ at time t, and all of them can be constructed from $\{\boldsymbol{x}_i\}_{i=1}^N$ through the following steps. In what follows, these are regarded as functions of time t with N-periodic index, i.e., $\mathsf{F}_0 = \mathsf{F}_N$, $\mathsf{F}_{N+1} = \mathsf{F}_1$.

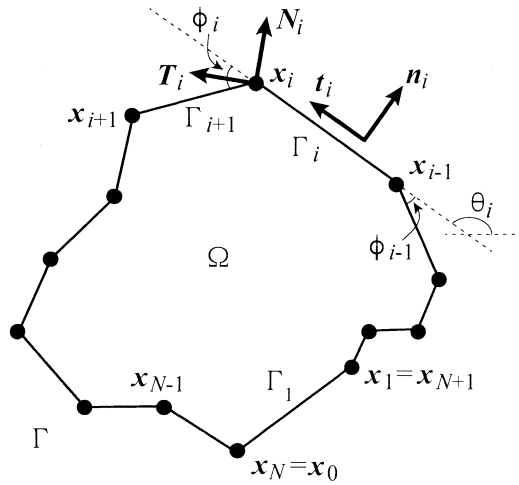

Figure 3.1: Moving Jordan polygonal curve

Step 1 several polygonal quantities (see Figure 3.1)

$r_i = |\boldsymbol{x}_i - \boldsymbol{x}_{i-1}|$: the length of Γ_i,

$L = \sum_{i=1}^{N} r_i$: the total length of Γ,

$\boldsymbol{t}_i = (\boldsymbol{x}_i - \boldsymbol{x}_{i-1})/r_i$: the unit tangent vector on Γ_i,

$\boldsymbol{n}_i = -\boldsymbol{t}_i^{\perp}$: the outward unit normal vector on Γ_i,

$\phi_i = \mathrm{sgn}(\det(\boldsymbol{t}_i, \boldsymbol{t}_{i+1}))\arccos(\boldsymbol{t}_i \cdot \boldsymbol{t}_{i+1})$: the angle between the adjacent edges Γ_i and Γ_{i+1},

$\boldsymbol{T}_i = (\boldsymbol{t}_i + \boldsymbol{t}_{i+1})/(2\mathsf{cos}_i)$: the unit tangent vector at $\boldsymbol{x}_i$, where $\mathsf{cos}_i = \cos(\phi_i/2)$,

$\boldsymbol{N}_i = -\boldsymbol{T}_i^{\perp}$: the unit outward normal vector at $\boldsymbol{x}_i$,

$\kappa_i = (\mathsf{tan}_i + \mathsf{tan}_{i-1})/r_i$: the curvature on Γ_i, where $\mathsf{sin}_i = \sin(\phi_i/2)$, $\mathsf{tan}_i = \mathsf{sin}_i/\mathsf{cos}_i$;

Step 2 the normal velocity $V_i = (v_i + v_{i+1})/(2\mathsf{cos}_i)$ at $\boldsymbol{x}_i$, where
v_i is a given averaged normal velocity on Γ_i such as $v_i = -\kappa_i$, and so on;

Step 3 the tangential velocity W_i at $\boldsymbol{x}_i$ is defined by one of the followings:

(1) Uniform Distribution Method: $W_i = (\Psi_i + c)/\mathsf{cos}_i$ at $\boldsymbol{x}_i$, where
$\Psi_i = \sum_{j=1}^{i} \psi_j$, $c = -\left(\sum_{j=1}^{N} \Psi_j/\mathsf{cos}_j\right) \Big/ \left(\sum_{j=1}^{N} \mathsf{cos}_j\right)$, $\psi_1 = 0$ and

$$\psi_j = \frac{1}{N}\sum_{l=1}^{N} \kappa_l v_l r_l - V_j \mathsf{sin}_j - V_{j-1}\mathsf{sin}_{j-1} + \left(\frac{L}{N} - r_j\right)\omega$$

for $j = 2, 3, \cdots, N$, and ω will be defined later;

(2) Crystalline Method: $W_i = (v_{i+1} - v_i)/(2\mathsf{sin}_i)$ at $\boldsymbol{x}_i$;

(3) Curvature Adjusted Method: an interpolation of (1) and (2);

GOAL (3.1) can be summarized as the following ODEs:

$$\dot{\boldsymbol{X}} = \boldsymbol{F}(\boldsymbol{X}), \tag{3.2}$$

where $\boldsymbol{X} = (\boldsymbol{x}_1, \boldsymbol{x}_2, \cdots, \boldsymbol{x}_N) \in \mathbb{R}^{2\times N}$, and

$$\begin{cases} \boldsymbol{F} = (\boldsymbol{F}_1, \boldsymbol{F}_2, \cdots, \boldsymbol{F}_N) : \mathbb{R}^{2\times N} \to \mathbb{R}^{2\times N}; \\ \mathbb{R}^{2\times N} \ni \boldsymbol{X} \mapsto \boldsymbol{F}_i(\boldsymbol{X}) \in \mathbb{R}^2 \ (i = 1, 2, \cdots, N). \end{cases}$$

The background of the above steps are the followings.

Step 1 Several polygonal quantities r_i, L, $\boldsymbol{t}_i$, $\boldsymbol{n}_i$ and ϕ_i are defined naturally as in Step 1.

- To define the tangent and normal vectors at $\boldsymbol{x}_i$, we use the angle ϕ_i between the adjacent edges Γ_i and Γ_{i+1} ($\boldsymbol{t}_i \cdot \boldsymbol{t}_{i+1} = \cos\phi_i$). As in Figure 3.1, the unit tangent vector $\boldsymbol{T}_i$ at $\boldsymbol{x}_i$ are defined by an average of the adjacent corresponding vectors in the sense as in Step 1.
- To define the curvatures on Γ_i and at $\boldsymbol{x}_i$, we use (2.2) rather than the Frenét formulae, i.e., we recall that the curvature can be defined by the first variation of the total length $\mathcal{L}$ from (2.2). From (3.1), the total length L, and $\dot{r}_i = V_i\mathsf{sin}_i + V_{i-1}\mathsf{sin}_{i-1} + W_i\mathsf{cos}_i - W_{i-1}\mathsf{cos}_{i-1}$, we obtain $\dot{L} = \sum_{i=1}^N \hat{\kappa}_i V_i \hat{r}_i$, where $\hat{r}_i = (r_i + r_{i+1})/2$, and $\hat{\kappa}_i = 2\mathsf{sin}_i/\hat{r}_i$ is the polygonal curvature at $\boldsymbol{x}_i$. It is a natural definition since the normal velocity V_i at $\boldsymbol{x}_i$ is the average of the adjacent normal averaged velocities in the sense of Step 2. Then it follows that

$$\dot{L} = \sum_{i=1}^N \kappa_i v_i r_i, \tag{3.3}$$

which is a discretization of (2.2), where κ_i in Step 1 is the polygonal curvature on Γ_i. Note that κ_i is same as the polygonal curvature or the crystalline curvature in a prescribed class of polygonal curves [2] and v_i is not necessarily equivalent to $\dot{\boldsymbol{x}}_i \cdot \boldsymbol{n}_i$ (see the next step (2)).

Step 3 Let L_ε be a small perturbation ε of L at $\boldsymbol{x}_i$ only such as $\boldsymbol{x}_i + \varepsilon\boldsymbol{z}$. The $\boldsymbol{z}$-directional derivative of L_ε is $dL_\varepsilon/d\varepsilon|_{\varepsilon=0} = \hat{\kappa}_i \boldsymbol{N}_i \cdot \boldsymbol{z}\hat{r}_i$. Hence $\boldsymbol{z} = -\boldsymbol{N}_i$ is the gradient direction of L at $\boldsymbol{x}_i$. However, from the enclosed area $A = \sum_{i=1}^N \boldsymbol{x}_{i-1}^\perp \cdot \boldsymbol{x}_i/2$, we have $dA_\varepsilon/d\varepsilon|_{\varepsilon=0} = \tilde{\boldsymbol{N}}_i \cdot \boldsymbol{z}$ with $\tilde{\boldsymbol{N}}_i = r_i\boldsymbol{n}_i + r_{i+1}\boldsymbol{n}_{i+1}$, and hence $\tilde{\boldsymbol{N}}_i$ is not the same direction as $\boldsymbol{N}_i$ unless $r_i \equiv L/N$. Therefore, $\boldsymbol{N}_i$ is not the gradient direction of A, and so an error term (comparing with (2.1)) appears as follows:

$$\dot{A} = \sum_{i=1}^N v_i r_i + \mathrm{err}_A, \quad \mathrm{err}_A = \sum_{i=1}^N \left(W_i\mathsf{sin}_i - \frac{v_{i+1} - v_i}{2} \right) \frac{r_{i+1} - r_i}{2}. \tag{3.4}$$

There are two ways to vanish err_A:

(1) To use W_i satisfying $r_i \equiv L/N$:
This method is called the uniform distribution method (UDM in short). Because of numerical errors, an asymptotic UDM is utilized practically as follows. To obtain the asymptotic UDM, $r_i \to L/N$ $(t \to T_{\max} \leq \infty)$, we assume that for $i = 1, 2, \cdots, N$

$$r_i - \frac{L}{N} = \eta_i e^{-\mu(t)} \quad \left(\sum_{i=1}^{N} \eta_i = 0, \ \lim_{t \to T_{\max}} \mu(t) = \infty \right).$$

Differentiating the both sides and putting $\omega(t) = \dot{\mu}(t)$, we have $\dot{r}_i = U_i$ for $i = 1, 2, \cdots, N$, where

$$U_i = \frac{\dot{L}}{N} + \left(\frac{L}{N} - r_i \right) \omega(t), \quad \int_0^{T_{\max}} \omega(t)\, dt = \infty,$$

and ω is a large value if $T_{\max} = \infty$ as in this paper's case, and we obtain the tangential velocity equation $W_i \mathsf{cos}_i - W_{i-1} \mathsf{cos}_{i-1} = U_i - V_i \mathsf{sin}_i - V_{i-1} \mathsf{sin}_{i-1}$ for $i = 1, 2, \cdots, N$. Since these N equations are linearly dependent, imposing the zero-average condition $\sum_{i=1}^{N} W_i = 0$ yields N linearly independent equations, which can be solved as in Step 3.

(2) To use $W_i = (v_{i+1} - v_i)/(2\mathsf{sin}_i)$:
This method is called crystalline method which is equivalent to the case $v_i = \dot{\boldsymbol{x}}_i \cdot \boldsymbol{n}_i$, and in this case, Γ is restricted in a prescribed class of polygonal curves as mentioned in Step 1.

(3) This method is an interpolation of (1) and (2) developed by [1, 13].

To solve ODEs (3.2), one can use the following several methods: the Euler method, a semi-implicit method, the classical fourth order Runge-Kutta method, and an iteration method, depending on each problem.

4 The Hele-Shaw flow equation in Example 2.6

The averaged normal velocity v_i in Step 2 will be approximated from the normal velocity of the Hele-Shaw flow equation (2.4) in Example 2.6, by means of the **Method of Fundamental Solutions** (**MFS** in short) as follows.

For each fixed $t \geq 0$ we solve the following Dirichlet problem:

$$\begin{cases} \triangle p = 0 & \text{in } \Omega(t), \\ p = \gamma \kappa_i & \text{on } \Gamma_i(t) \quad (i = 1, 2, \cdots, N). \end{cases}$$

We seek the approximate solution P of the form

$$P(\boldsymbol{x}) = Q_0 + \sum_{j=1}^{N} Q_j E_j(\boldsymbol{x}), \quad E_j(\boldsymbol{x}) := E(\boldsymbol{x} - \boldsymbol{y}_j) - E(\boldsymbol{x} - \boldsymbol{z}_j) \quad (\boldsymbol{x} \in \overline{\Omega}(t)), \tag{4.1}$$

$$P(\boldsymbol{x}_i^*) = \gamma \kappa_i \quad (i = 1, 2, \cdots, N), \tag{4.2}$$

$$v_i = -\nabla P(\boldsymbol{x}_i^*) \cdot \boldsymbol{n}_i \quad (i = 1, 2, \cdots, N), \tag{4.3}$$

where $E(\boldsymbol{x}) = \log|\boldsymbol{x}|/(2\pi)$ is the fundamental solution of the Laplace operator $\triangle$, $\boldsymbol{x}_i^* = (\boldsymbol{x}_i + \boldsymbol{x}_{i-1})/2$ is the mid point on Γ_i, $\{Q_j\}_{j=0}^N$ are unknown coefficients which will be solved below, $\boldsymbol{y}_j$'s are the singular points defined by

$$\boldsymbol{y}_j = \boldsymbol{x}_j^* + d\boldsymbol{n}_j \quad (j = 1, 2, \cdots, N),$$

where $d > 0$ is a parameter controlling accuracy of MFS, and $\boldsymbol{z}_j$'s are "dummy" points located in $\mathbb{R}^2 \backslash \overline{\Omega}(t)$ which are not equal to the singular points $\{\boldsymbol{y}_j\}_{j=1}^N$.

Note that P satisfies $\triangle P = 0$ in Ω and is invariant under the trivial affine transformation and the origin shift of the boundary data as well as the original invariant scheme of MFS or so-called the Charge Simulation Method (see [12] and references therein). One can add one more condition which is required for the invariance of the original invariant scheme of MFS. We select the condition such a way that the weighted average of Q_j's is equal to 0, that is, coefficients $\{Q_j\}_{j=0}^N$ are determined by (4.2) and

$$\sum_{j=1}^{N} Q_j H_j = 0, \quad H_j = -\sum_{i=1}^{N} \nabla E_j(\boldsymbol{x}_i^*) \cdot \boldsymbol{n}_i r_i, \quad j = 1, 2, \cdots, N. \tag{4.4}$$

One can solve this system of $N+1$ linear equations (4.2) and (4.4) by a standard elimination method.

As mentioned in Example 2.6, AP-property and CS-property hold for Hele-Shaw problem. When the averaged normal velocity v_i on Γ_i is defined by (4.3), if $\mathrm{err}_A = 0$ by UDM, then we have

$$\dot{A} = \sum_{i=1}^{N} v_i r_i = \sum_{j=1}^{N} Q_j H_j = 0, \tag{4.5}$$

where H_j's are in (4.4). Thus AP-property holds in a discrete sense.

We also have the approximated CS-property as follows.

$$\begin{aligned}
\dot{L} &= \sum_{i=1}^{N} \kappa_i v_i r_i = -\sum_{i=1}^{N} \kappa_i \nabla P(\boldsymbol{x}_i^*) \cdot \boldsymbol{n}_i r_i = -\frac{1}{\gamma} \sum_{i=1}^{N} P(\boldsymbol{x}_i^*) \nabla P(\boldsymbol{x}_i^*) \cdot \boldsymbol{n}_i r_i \\
&= -\frac{1}{\gamma} \sum_{i=1}^{N} \int_{\Gamma} P(\boldsymbol{x}_i^*) \nabla P(\boldsymbol{x}_i^*) \cdot \boldsymbol{n}_i \, ds \\
&\approx -\frac{1}{\gamma} \sum_{i=1}^{N} \int_{\Gamma_i} P(\boldsymbol{x}) \nabla P(\boldsymbol{x}) \cdot \boldsymbol{n}_i \, ds = -\frac{1}{\gamma} \int_{\Gamma} P(\boldsymbol{x}) \nabla P(\boldsymbol{x}) \cdot \boldsymbol{n} \, ds \\
&= -\frac{1}{\gamma} \iint_{\Omega} \mathrm{div}(P \nabla P) \, dxdy = -\frac{1}{\gamma} \iint_{\Omega} |\nabla P|^2 \, dxdy \le 0.
\end{aligned}$$

Note that, instead of (4.2) and (4.3), if we use

$$[P]_i = \gamma \kappa_i, \quad i = 1, 2, \cdots, N, \tag{4.6}$$

$$v_i = -\langle \nabla P \rangle_i \cdot \boldsymbol{n}_i, \quad i = 1, 2, \cdots, N, \tag{4.7}$$

where $\langle \mathsf{F} \rangle_i = r_i^{-1} \int_{\Gamma_i} \mathsf{F} \, ds$ is the average of F on Γ_i, and $[\mathsf{F}]_i = \langle \mathsf{F} \nabla \mathsf{F} \rangle_i \cdot \boldsymbol{n}_i / \langle \nabla \mathsf{F} \rangle_i \cdot \boldsymbol{n}_i$, then we have $\dot{L} \le 0$ without an approximation. However, in this case we have to solve nonlinear $N+1$ equations of $\{Q_j\}_{j=0}^N$, and that computational cost is not cheap.

To solve ODEs (3.2), we use the classical fourth order Runge-Kutta method. A precise argument and several numerical experiments can be found in [11].

5 The area-preserving crystalline curvature flow equation in Example 2.7

In the crystalline setting, we use the following additional polygonal quantities (cf. §3):

Step 1 (addition)

$h_i = \boldsymbol{x}_i \cdot \boldsymbol{n}_i = \boldsymbol{x}_{i-1} \cdot \boldsymbol{n}_i$: the hight function for Γ_i,

θ_i: the tangent angle satisfying $\boldsymbol{t}_i = (\cos\theta_i, \sin\theta_i)^{\mathrm{T}}$. See Figure 3.1. All tangent angles $\{\theta_i\}_{i=0}^{N+1}$ can be derived as in the following procedure: Firstly, from $\boldsymbol{t}_1 = (t_{11}, t_{12})^{\mathrm{T}}$, we have $\theta_1 = -\arccos(t_{11})$ if $t_{12} < 0$; $\theta_1 = \arccos(t_{11})$ if $t_{12} \geq 0$. Secondly, for $i = 1, 2, \cdots, N$, we successively compute θ_{i+1} from θ_i as $\theta_{i+1} = \theta_i + \phi_i$. Finally, we obtain $\theta_0 = \theta_1 - (\theta_{N+1} - \theta_N)$, since $\theta_N = \theta_0 + 2\pi$ and $\theta_{N+1} = \theta_1 + 2\pi$ hold.

Note that all the polygonal quantities above and in Step 1 except $\{\theta_i\}_{i=0}^{N+1}$ satisfy the periodic boundary conditions: $\mathsf{F}_0 = \mathsf{F}_N$, $\mathsf{F}_{N+1} = \mathsf{F}_1$.

Construction $(h, \nu \Rightarrow \boldsymbol{x}, \boldsymbol{t}, \boldsymbol{n}, r)$**.** The set of vertices $\{\boldsymbol{x}_i\}_{i=1}^{N}$ can be constructed from the sets $\{h_i\}_{i=1}^{N+1}$ $(h_{N+1} = h_1)$ and $\{\theta_i\}_{i=1}^{N+1}$ $(\theta_{N+1} = \theta_1 + 2\pi)$ as follows. Let $\boldsymbol{t}(\theta) = (\cos\theta, \sin\theta)^{\mathrm{T}}$ and $\boldsymbol{n}(\theta) = (\sin\theta, -\cos\theta)^{\mathrm{T}}$, and then we have $\boldsymbol{t}_i = \boldsymbol{t}(\theta_i)$ and $\boldsymbol{n}_i = \boldsymbol{n}(\theta_i)$. Since $h_i = \boldsymbol{x}_i \cdot \boldsymbol{n}(\theta_i)$ and $h_{i+1} = \boldsymbol{x}_i \cdot \boldsymbol{n}(\theta_{i+1})$, from the sets $\{h_i\}_{i=1}^{N+1}$ and $\{\theta_i\}_{i=1}^{N+1}$ we obtain $\boldsymbol{x}_i = (h_{i+1}\boldsymbol{t}_i - h_i\boldsymbol{t}_{i+1})/\sin\phi_i$ for $i = 1, 2, \cdots, N$. From this the length of the i-th edge can be described as

$$r_i = \frac{h_{i+1}}{\sin\phi_i} - h_i(\cot\phi_i + \cot\phi_{i-1}) + \frac{h_{i-1}}{\sin\phi_{i-1}}.$$

For N-tuples $\boldsymbol{h} = (h_1, h_2, \cdots, h_N)$ and $\boldsymbol{\phi} = (\phi_1, \phi_2, \cdots, \phi_N)$ with the periodic boundary conditions $\mathsf{F}_0 = \mathsf{F}_N, \mathsf{F}_{N+1} = \mathsf{F}_1$, we denote the right hand side of r_i as $D_i(\boldsymbol{h}, \boldsymbol{\phi})$, i.e., $r_i = D_i(\boldsymbol{h}, \boldsymbol{\phi})$ holds for $i = 1, 2, \cdots, N$.

The Wulff polygon and admissibility. Now let us restrict the polygonal curve Γ in an admissible class associated with the N_σ-sided convex polygon, say the Wulff polygon $\mathcal{W}_\sigma$ for an appropriate positive function σ: $\mathcal{W}_\sigma = \bigcap_{i=1}^{N_\sigma}\{\boldsymbol{x} \in \mathbb{R}^2;\, \boldsymbol{x} \cdot \boldsymbol{n}(\eta_i) \leq \sigma(\eta_i)\}$, where η_i is the tangent angle of the i-th edge of $\mathcal{W}_\sigma$ $(i = 1, 2, \cdots, N_\sigma)$. Such σ is called crystalline interfacial energy density. The length of the i-th edge is described as $l_\sigma(\eta_i) = D_i(\boldsymbol{\sigma}(\eta), \boldsymbol{\psi})$, where $\boldsymbol{\sigma}(\eta) = (\sigma(\eta_1), \sigma(\eta_2), \cdots, \sigma(\eta_{N_\sigma}))$, $\boldsymbol{\psi} = (\psi_1, \psi_2, \cdots, \psi_{N_\sigma})$, and $\psi_i = \eta_{i+1} - \eta_i \in (0, \pi)$ for $i = 1, 2, \cdots, N_\sigma$ $(\psi_0 = \psi_{N_\sigma},\ \psi_{N_\sigma+1} = \psi_1)$. Note that $\sigma > 0$ should be satisfied $l_\sigma(\eta_i) > 0$ for $i = 1, 2, \cdots, N_\sigma$. Let $\mathcal{N} = \{\boldsymbol{n}_i\}_{i=1}^{N}$ and $\mathcal{N}_\sigma = \{\boldsymbol{n}(\eta_j)\}_{j=1}^{N_\sigma}$ be the set of normal vectors on Γ and $\partial\mathcal{W}_\sigma$, respectively. The polygonal curve Γ is called $\mathcal{W}_\sigma$-admissible if the following two conditions are satisfied.

$$(1)\ \mathcal{N} \subset \mathcal{N}_\sigma; \quad (2)\ \frac{(1-\lambda)\boldsymbol{n}_i + \lambda\boldsymbol{n}_{i+1}}{|(1-\lambda)\boldsymbol{n}_i + \lambda\boldsymbol{n}_{i+1}|} \notin \mathcal{N}_\sigma \quad (i = 1, 2, \cdots, N; \boldsymbol{n}_{N+1} = \boldsymbol{n}_1; \lambda \in (0, 1)).$$

Let $\Gamma(t)$ be the $\mathcal{W}_\sigma$-admissible, N-sided and time t-dependent polygonal curve. The curve $\Gamma(t) = \bigcup_{i=1}^{N}\Gamma_i(t)$, $\Gamma_i(t) = [\boldsymbol{x}_{i-1}(t), \boldsymbol{x}_i(t)]$ evolves by prescribed normal velocities:

$$v_i = \dot{\boldsymbol{x}}_i \cdot \boldsymbol{n}(\theta_i) = \dot{h}_i \quad (i = 1, 2, \cdots, N),$$

which will be defined later. Note that for any ϕ_i there is a $j \in \{1, 2, \cdots, N_\sigma\}$ such that $|\phi_i| = \psi_j$ holds.

The energy and the crystalline curvature. The total interfacial crystalline energy is defined by $L_\sigma = \sum_{i=1}^N \sigma(\theta_i) r_i$. Since the time differential of $r_i = D_i(\boldsymbol{h}, \boldsymbol{\phi})$ is $\dot{r}_i = D_i(\dot{\boldsymbol{h}}, \boldsymbol{\phi}) = D_i(\boldsymbol{v}, \boldsymbol{\phi})$, where $\boldsymbol{v} = (v_1, \cdots, v_N)$, the time differential of L_σ is

$$\dot{L}_\sigma = \sum_{i=1}^N \sigma(\theta_i) D_i(\boldsymbol{v}, \boldsymbol{\phi}) = \sum_{i=1}^N v_i D_i(\boldsymbol{\sigma}(\theta), \boldsymbol{\phi}) = \sum_{i=1}^N \kappa_{\sigma i} v_i r_i,$$

where $\kappa_{\sigma i} = D_i(\boldsymbol{\sigma}(\theta), \boldsymbol{\phi})/r_i$, $D_i(\boldsymbol{\sigma}(\theta), \boldsymbol{\phi}) = \chi_i l_\sigma(\theta_i)$, $\chi_i = (\mathrm{sgn}(\phi_{i-1}) + \mathrm{sgn}(\phi_i))/2$, $\boldsymbol{\sigma}(\theta) = (\sigma(\theta_1), \sigma(\theta_2), \cdots, \sigma(\theta_N))$. The $\kappa_{\sigma i}$ is called the i-th crystalline curvature, and the χ_i is called the i-th transition number.

The gradient flow subject to area-preserving. The time differential of enclosed area $A = \sum_{i=1}^N h_i r_i/2$ is $\dot{A} = \sum_{i=1}^N v_i r_i$ without the error term err_A, since the tangential velocity is given by (2) Crystalline Method in Step 2. As the area-preserving gradient flow of L_σ, we obtain the area-preserving crystalline curvature flow equations

$$v_i = \langle \kappa_\sigma \rangle - \kappa_{\sigma i}, \quad \langle \mathsf{F} \rangle = \frac{1}{L} \sum_{i=1}^N \mathsf{F}_i r_i \quad (i = 1, 2, \cdots, N). \tag{5.1}$$

Now we are ready to set up the problem. Let P_σ^N be a set of all $\mathcal{W}_\sigma$-admissible, N-sided polygonal Jordan curve in the plane. For a given $\Gamma^0 \in P_\sigma^N$ find a family of curves $\{\Gamma(t) \in P_\sigma^N\}_{0 \le t < T}$ satisfying $\dot{h}_i = v_i$ $(i = 1, 2, \cdots, N)$, starting from $\Gamma(0) = \Gamma^0$.

An iteration. Instead of solving ODEs (3.2), we solve the equivalent ODEs $\dot{h}_i = v_i$ by the following discretization

$$\frac{h_i^{m+1/2} - h_i^m}{\tau_m/2} = F_i(\boldsymbol{h}^{m+1/2}) = \frac{\sum_{j=1}^N k_{\sigma j}^{m+1/2} r_j^{m+1/2}}{\sum_{j=1}^N r_j^{m+1/2}} - k_{\sigma i}^{m+1/2},$$

where $k_{\sigma i}^{m+1/2} = D_i(\boldsymbol{\sigma}(\nu^m), \boldsymbol{\phi}^m)/r_i^{m+1/2}$, $r_i^{m+1/2} = D_i(\boldsymbol{h}^{m+1/2}, \boldsymbol{\phi}^m)$, and solve this by the iteration as in the following steps.

(1) $l = 0$; $\boldsymbol{y}^{(l)} = \boldsymbol{h}^m$;

(2) $\boldsymbol{y}^{(l+1)} = \boldsymbol{h}^m + \boldsymbol{F}(\boldsymbol{y}^{(l)})\tau_m/2$;

(3) If $||\boldsymbol{y}^{(l+1)} - \boldsymbol{y}^{(l)}||/r_{\max}^m \le \delta_{\mathrm{tol}}$, then GOTO (5);

(4) $l := l + 1$; GOTO (2);

(5) $\boldsymbol{h}^{m+1} = R^{(l+1)} \widetilde{\boldsymbol{y}}^{(l+1)}$, $\widetilde{\boldsymbol{y}}^{(l+1)} = 2\boldsymbol{y}^{(l+1)} - \boldsymbol{h}^m$, $R^{(l+1)} = \sqrt{A^0/\widetilde{A}^{(l+1)}}$.

Here $\delta_{\mathrm{tol}} > 0$ is a tolerance, A^0 is the enclosed area of Γ^0, $\widetilde{A}^{(j)}$ is the enclosed area of a polygon constructed from the heights $\{\widetilde{y}_i^{(j)}\}_{i=1}^N$, $\boldsymbol{y}^{(j)} = (y_1^{(j)}, \cdots, y_N^{(j)})$, $\boldsymbol{F}(\boldsymbol{y}^{(j)}) = (F_1(\boldsymbol{y}^{(j)}), \cdots, F_N(\boldsymbol{y}^{(j)}))$, $\widetilde{\boldsymbol{y}}^{(j)} = (\widetilde{y}_1^{(j)}, \cdots, \widetilde{y}_N^{(j)})$, $||\boldsymbol{y}^{(l+1)} - \boldsymbol{y}^{(l)}|| = \max_{1 \le i \le N} |y_i^{(l+1)} - y_i^{(l)}|$, and $\mathsf{F}_{\max} = \max_{1 \le i \le N} \mathsf{F}_i$.

The iteration succeeds in showing the convergence $\lim_{l \to \infty} y_i^{(l)} = h_i^{m+1}$, the AP-property $A^{m+1} = A^m$ and the energy-decaying property $L_\sigma^{m+1} \le L_\sigma^m$. See [2, 6].

6 The closed curve version of the Kuramoto-Sivashinsky equation in Example 2.8

To approximate (2.6), κ_{ss} is discretized as follows.

Step 1 (addition) $(\kappa_{ss})_i = ((\kappa_{\hat{s}})_{i+1} - (\kappa_{\hat{s}})_{i-1})/(2r_i)$, where

$$(\mathsf{F}_{\hat{s}})_i = \frac{1}{r_i}\left(\frac{\mathsf{F}_{i+1}+\mathsf{F}_i}{2\mathsf{cos}_i^2} - \frac{\mathsf{F}_i+\mathsf{F}_{i-1}}{2\mathsf{cos}_{i-1}^2}\right) \quad \text{on} \quad \Gamma_i. \tag{6.1}$$

Then the averaged normal velocity on Γ_i can be defined as $v_i = v^{(0)} + (\alpha_{\mathrm{eff}} - 1)\kappa_i + \delta(\kappa_{ss})_i$, $v^{(0)} = V^{(0)}$.

To compute $(\kappa_{ss})_i$, we calculate the gradient flow of $E = \sum_{i=1}^{N} \kappa_i^2 r_i/2$, which is a discrete analogue for obtaining the Willmore flow equation from (2.3). Under a direct calculation, we have

$$\dot{E} = -\sum_{i=1}^{N}\left((\kappa_{ss})_i + \frac{1}{2}\langle\kappa^3\rangle_i\right) v_i r_i + \mathrm{err}_E, \tag{6.2}$$

where $\langle\kappa^3\rangle_i = (\kappa_i^+\kappa_{i+1}^2 + 2\kappa_i^3 + \kappa_i^-\kappa_{i-1}^2)/4$ is an average of κ_i cubed on Γ_i ($\kappa_i^+ = 2\mathsf{tan}_i/r_i$, $\kappa_i^- = 2\mathsf{tan}_{i-1}/r_i$, n.b. $\kappa_i = (\kappa_i^+ + \kappa_i^-)/2$), and err_E is the remaining term.

The term $(\kappa_{ss})_i$ is extracted from (6.2). Note that the difference operator (6.1) is meaningful, since $(\boldsymbol{t}_{\hat{s}})_i = -\kappa_i \boldsymbol{n}_i$ holds, which is a discrete version of the Frenét formula $\boldsymbol{T}_s = -\kappa \boldsymbol{N}$. Of course, this argument is not the only way to obtain κ_{ss}, for example, $\boldsymbol{x}_{ssss}$ based method is also valid [10].

To solve ODEs (3.2), we use the classical fourth order Runge-Kutta method. A precise argument and several numerical experiments can be found in [3].

7 Conclusion

We showed a simple and fast numerical method for a general moving boundary problems, and especially for the classical Hele-Shaw problem, the area-preserving crystalline curvature flow equation, and the closed curve version of Kuramoto-Sivashinsky equation.

References

[1] M. Beneš, M. Kimura, D. Ševčovič, T. Tsujikawa and S. Yazaki, Application of a curvature adjusted method in image segmentation, *Bull. Inst. Math. Acad. Sin. (New Series)* **3** (2008) 509–523.

[2] M. Beneš, M. Kimura and S. Yazaki, Second order numerical scheme for motion of polygonal curves with constant area speed, *Interfaces Free Bound.* **11** (2009) 515–536.

[3] M. Goto, K. Kuwana and S. Yazaki, A simple and fast numerical method for solving flame/smoldering evolution equations, *Submitted.*

[4] B. Gustafsson & A. Vasil'ev, *Conformal and Potential Analysis in Hele-Shaw Cells*, Birkhaeuser (2006).

[5] H. S. Hele-Shaw, The flow of water, *Nature* **58** (1898) 34–36, 520.

[6] T. Ishiwata & S. Yazaki, Structure-preserving numerical scheme for a generalized area-preserving crystalline curvature flow, *Computer Methods in Materials Science* **17** (2017) 122–135; Convexity phenomena arising in an area-preserving crystalline curvature flow –Nakaya's observation and its mathematical justification, *Submitted.*

[7] Y. Kuramoto & T. Tsuzuki, Persistent propagation of concentration waves in dissipative media far from thermal equilibrium, *Progress of Theoretical Physics* **55** (1976) 356–369.

[8] H. Lamb, *Hydrodynamics*, 6th edition, Dover Publications (1945).

[9] K. Mikula & D. Ševčovič, A direct method for solving an anisotropic mean curvature flow of plane curves with an external force, *Math. Methods Appl. Sci.* **27** (2004) 1545–1565; Computational and qualitative aspects of evolution of curves driven by curvature and external force, *Comput. and Vis. in Science* **6** (2004) 211–225; Evolution of curves on a surface driven by the geodesic curvature and external force, *Applicable Analysis* **85** (2006) 345–362.

[10] K. Mikula, D. Ševčovič and M. Balažovjech, A Simple, Fast and Stabilized Flowing Finite Volume Method for Solving General Curve Evolution Equations, *Commun. Comput. Phys.* **7** (2010) 195–211.

[11] K. Sakakibara & S. Yazaki, A charge simulation method for the computation of Hele-Shaw problems, *RIMSK* **1957** (2015) 116–133; Structure-preserving numerical scheme for the one-phase Hele-Shaw problems by the method of fundamental solutions, *Submitted.*

[12] K. Sakakibara & S. Yazaki, On invariance of schemes in the method of fundamental solutions, *Appl. Math. Lett.* **73** (2017) 16–21; Method of fundamental solutions with weighted average condition and dummy points, *JSIAM Lett.* **9** (2017) 41–44.

[13] D. Ševčovič & S. Yazaki, Evolution of plane curves with a curvature adjusted tangential velocity, *Jpn. J. Ind. Appl. Math.* **28** (2011) 413–442; Computational and qualitative aspects of motion of plane curves with a curvature adjusted tangential velocity, *Mathematical Methods in the Applied Sciences* **35** (2012) 1784–1798.

[14] D. Ševčovič & S. Yazaki, On a gradient flow of plane curves minimizing the anisoperimetric ratio, *IAENG International Journal of Applied Math.* **43** (2013) 160–171.

[15] G. I. Sivashinsky, Nonlinear analysis of hydrodynamic instability in laminar flames–I. Derivation of basic equations, *Acta Astronautica* **4** (1977) 1177–1206.